Vol. 712: 67–85, 2023
https://doi.org/10.3354/meps14317

MARINE ECOLOGY PROGRESS SERIES
Mar Ecol Prog Ser

Published June 8

Alaska deep-sea coral and sponge assemblages are well-defined and mostly predictable from local environmental conditions

Michael F. Sigler[1,#,*], Christopher N. Rooper[2,#], Pam Goddard[3], Rachel Wilborn[3], Kresimir Williams[3]

[1]Shoals Marine Laboratory, Isles of Shoals, Maine, USA, and National Oceanic and Atmospheric Administration, National Marine Fisheries Service, Alaska Fisheries Science Center (retired), 17109 Point Lena Loop Road, Juneau, AK 99801-8626, USA
[2]Pacific Biological Station, Fisheries and Oceans Canada (DFO), 3190 Hammond Bay Road, Nanaimo, BC V9T 6N7, Canada
[3]National Oceanic and Atmospheric Administration, National Marine Fisheries Service, Alaska Fisheries Science Center, Resource Assessment and Conservation Engineering Division, 7600 Sand Point Way NE, Seattle, WA 98115-6349, USA

ABSTRACT: Vulnerable marine ecosystems (VMEs), including deep-sea corals and sponges, are important habitats for many fish and invertebrate species and are at risk from the effects of fishing, seafloor mining, and climate change. We describe the zoogeography of deep-sea corals and sponges in Alaska, USA, and identify the environmental factors structuring these assemblages. Images were collected with a calibrated stereo drop-camera (n = 853 transect locations). We used cluster analysis to identify assemblages, canonical correspondence analysis to identify the primary environmental variables structuring these assemblages, and random forest and generalized additive modeling to predict their spatial distributions. The 6 identified assemblages were well defined, with each dominated by a single indicator taxon (2 coral taxa: Primnoidae, Stylasteridae; 2 sponge taxa: Demospongiae, Hexactinellida; 2 sea whip/pen taxa: *Balticina* sp., *Ptilosarcus gurneyi*). The most common assemblages were Demospongiae, Primnoidae, and *Balticina* sp. Primnoidae and Demospongiae were positively influenced by greater maximum tidal current, bottom current, and bottom temperature as well as proportion of rock and cobble (high for Primnoidae; low to medium for Demospongiae). *Balticina* sp. was influenced in the opposite direction and was aligned along lower maximum tidal current, bottom current, and bottom temperature as well as unconsolidated sediment and greater depth. We defined VME community indicators as the 6 assemblages, each dominated by a single indicator taxa. These VME community indicators can guide the identification of protected areas.

KEY WORDS: Coral · Sponge · Assemblage · Indicator taxa · Alaska

1. INTRODUCTION

Deep-sea corals and sponges are important benthic ecosystem components that provide complex 3-dimensional structure on the seafloor and are hotspots of biodiversity and abundance for marine fish and invertebrates (Buhl-Mortensen et al. 2010, Watling et al. 2011, Linley et al. 2017). In general, deep-sea corals and sponges are long-lived, slow to mature, have low reproductive output, and are structurally fragile, making them vulnerable to damage from fishing gear (Freese 2001, Koslow et al. 2001, Clark & Rowden 2009, Heifetz et al. 2009). Structured habitats are preferred by many fish species (e.g. *Sebastes* spp.), and deep-sea corals and sponges can form structure on otherwise featureless seafloor (Brodeur 2001, Love et al. 2006, Rooper et al. 2018). Vulnerable marine ecosystems (VMEs) are

[#] These authors contributed equally
[*] Corresponding author: mikesigler8@gmail.com

areas where fishing activities are likely to have deleterious impacts on the benthic community (FAO 2009). In 2006, the UN General Assembly resolution 61/105 adopted language to prevent impacts on VMEs by deep-sea fisheries by identifying areas where VMEs are known or likely to occur.

One difficulty with identifying areas where VMEs occur is that as a community, deep-sea corals and sponges are a large taxonomic grouping with varied life histories and habitat preferences (Stone et al. 2011, Wilborn et al. 2018). Taxonomic revisions are common in some taxonomic groups, such as sponges and alcyonacean corals (e.g. Cairns 2011, Reiswig 2020, McFadden et al. 2022). Identification of deep-sea corals and sponges can also be limited by the quality of images or field collections (e.g. McIntyre et al. 2016). Even for physically collected samples, sponge taxonomy is challenging and often requires microscopic examination of spicules to confirm identification to species. For these reasons, deep-sea corals and sponges are often treated at higher taxonomic levels such as order or class, or alternatively, indicator taxa are used to represent the distribution or presence of VMEs (FAO 2016, Jansen et al. 2018, Winship et al. 2020). Indicator taxa can be useful in that they can simplify the problem of large and heterogeneous groupings and allow monitoring of a series of single or easily identified taxa.

Environmental conditions influence where deep-sea corals and sponges are found. In the deep-sea area of Porcupine Bight, northeastern Atlantic Ocean, dense aggregations of sponges have been observed in areas adjacent to areas of high current speeds (Rice et al. 1990, White 2003). In Alaska, USA, upright sponges inhabit a variety of substrates, especially exposed rock with little sedimentation but also flat silty seafloors possibly with hard substrate beneath (Freese 2001), whereas corals usually inhabit hard substrates such as boulders and exposed bedrock (Cimberg et al. 1981, Krieger 2001) and are infrequently found on sandy or silty seafloors. Recruitment and abundance of corals and sponges may be influenced by the presence of exposed hard substrate (Gotelli 1988, Leys & Lauzon 1998). While other corals (e.g. Primnoidae) are largely found in rocky, shallower areas, sea whips typically occupy deeper depths and mostly unconsolidated substrates in Alaska (Wilborn et al. 2018).

Zoogeography is the study of the relationships among organisms living together and the environmental conditions that structure these relationships. Here, we examined the zoogeography of deep-sea corals and sponges in Alaska, identified assemblages and indicator taxa of these assemblages, and used a large set of several hundred observations to do so. After first identifying assemblages, we then identified the environmental factors structuring these assemblages and predicted their spatial distributions. This 'assemblage first–predict later' approach to identify and then model the distribution of biological communities has been frequently used in terrestrial ecosystems (Ferrier & Guisan 2006) and also applied to marine ecosystems (e.g. Moritz et al. 2013, Serrano et al. 2017, de la Torriente et al. 2019). Our study objectives were to (1) identify the major Alaska coral and sponge assemblages, (2) identify the environmental variables structuring these assemblages, (3) predict the spatial distributions of these assemblages and their indicator taxa, and (4) identify indicator taxa for VMEs and their conservation.

2. MATERIALS AND METHODS

2.1. Study area

The study area includes the eastern Bering Sea, Aleutian Islands region, and Gulf of Alaska (Fig. 1). The data set is extensive (n = 853 transect locations) and draws from nearly a decade (2010–2017) of fieldwork. Sampling designs included stratified random sampling of a region (e.g. eastern Bering Sea and Aleutian Islands; Rooper et al. 2014, 2016), haphazard random sampling of a region (e.g. sampling piggybacked on hydroacoustic surveys of the Gulf of Alaska), and random sampling of a few small areas (e.g. Habitat Area of Particular Concern sampling in the western Gulf of Alaska). Images were collected with a calibrated stereo drop-camera (Williams et al. 2010) deployed from a vessel that drifted or drove above the seafloor, usually for 15 min (targeted on-bottom time), where the distance traveled along the seafloor (mean ± SD: 380 ± 252 m) and the swath width (typically 2–5 m) were measured, and the camera was held 1–2 m from the seafloor (for more detail, see for example Rooper et al. 2016). Deployments for the Habitat Area of Particular Concern sampling were shorter, typically 5 min, and as short as 2 min over sandy seafloor. The seafloor area observed at a transect location averaged 1212 ± 905 m^2, and was as small as 14 m^2 during a 2 min deployment in a sandy, low-current area and as high as 7837 m^2 for a 15 min deployment in a high-current area. Each transect location (site) was sampled by a single camera deployment. Images were collected at 1 s intervals along the transect.

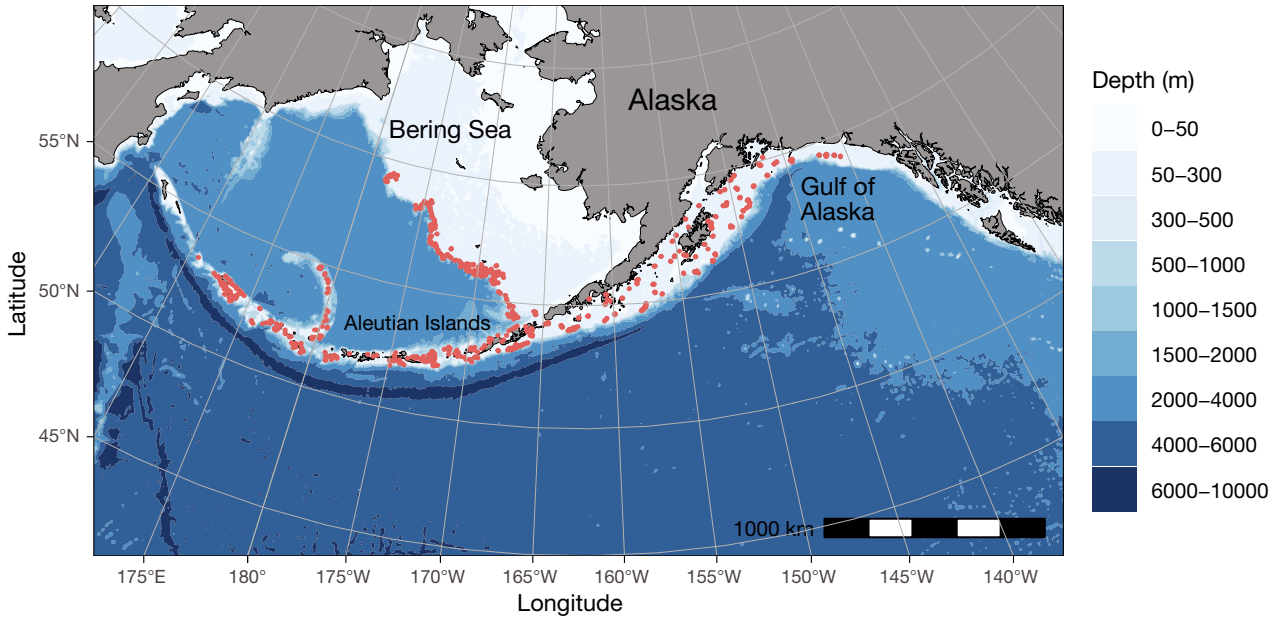

Fig. 1. Study area in the eastern Bering Sea, Aleutian Islands region, and the Gulf of Alaska. Red circles: transect locations (n = 853). Created using the R package ggOceanMaps (Vihtakari 2022)

2.2. Deep-sea coral and sponge data

Post-cruise image analysis was conducted to determine substrate types and deep-sea coral and sponge density at each site. All structure-forming invertebrates (corals, sponges, sea whips, and sea pens) were identified to the lowest possible taxonomic level and counted for each transect. The lowest identifiable taxonomic level was typically genus or species for corals and sea whips and order for sponges (Stone et al. 2011, Stone 2014). Although sea whips *Balticina* sp. and sea pens *Ptilosarcus gurneyi* are in the subclass containing corals (Octocorallia), they were considered separately from other corals in the suborders Holaxonia (family Plexauridae) and Calcaxonia (families Primnoidae and Isididae) because sea whips and sea pens prefer sandy, unconsolidated substrates whereas other corals prefer rocky substrate (cobble, boulder, or exposed bedrock).

The deep-sea coral and sponge data were aggregated to the finest consistently identified taxa, which comprised 12 groups (see Table 2). For example, the coral family Primnoidae could sometimes be identified to species (e.g. *Plumarella aleutiana*, 0.1% of cases) or genus (e.g. *Plumarella* sp., 27% of cases) in the post-cruise image analysis but in other cases could only be identified to family (Primnoidae, 64% of cases). Rather than have 2 overlapping taxa, we aggregated these observations into Primnoidae, which is the finest consistently identified taxa for these observations. In practice, only 3 of the 12 groups (all coral families) — Primnoidae, Plexauridae, and Acanthogorgiidae — were treated this way. Observations of *Fanellia* sp., *Plumarella aleutiana*, *Plumarella* sp., *Primnoa pacifica*, Primnoidae, and *Thouarella* sp. were grouped into Primnoidae, observations of *Alaskagorgia aleutiana*, *Muriceides* sp., Plexauridae, and *Swiftia* sp. were grouped into Plexauridae, and observations of *Acanthogorgia* sp., Acanthogorgiidae, and *Calcigorgia* sp. were grouped into Acanthogorgiidae. The remaining 9 taxa were consistently identified at the same resolution (e.g. no subgroupings of Demospongiae were identified). Four coarse identifications — Porifera (e.g. includes the sponge taxa Hexactinellida, Demospongiae, and Calcarea), coral, Octocorallia (includes several families but most likely were Primnoidae and Plexauridae), and Pennatuloidea (includes *Balticina* sp. and *P. gurneyi*) — overlap many of the finest-level consistently identified taxa but infrequently occurred (frequency of occurrence [FO] of 0.012, 0.002, 0.020, and 0.008, respectively). To avoid overlap, we excluded these 4 taxa from the analysis. As a result, we analyzed 12 taxa that formed mutually exclusive groups (see Table 2).

2.3. Environmental data

In total, 9 environmental variables (depth, slope, proportion of rock and cobble, bottom current, bottom temperature, maximum tidal current, ocean

color, aspect, and topographic position index [TPI]) were tested for their influence on structuring deep-sea coral and sponge assemblages. These variables were chosen based on their importance in determining coral and sponge distributions from previous analyses of Alaska deep-sea coral and sponge data (Rooper et al. 2014, 2016, Sigler et al. 2015).

Depth was collected during each camera deployment from either a SeaBird SBE-39 micro bathythermograph attached to the stereo-camera system or a housing-integrated calibrated pressure transducer. Start and end positions for the vessel during the on-bottom portion of each transect were collected using the vessel-mounted GPS receiver. The midpoint of the start and end positions was used as the location variable for longitude and latitude in the analysis. The longitude and latitude data for each transect (and all other geographical data including the raster layers described below) were projected into an Alaska Albers Equal Area Conic projection (center latitude: 50° N; center longitude: 154° W).

For each stereo-camera transect, the bottom substrate type was classified by a commonly used seafloor substratum classification system (Stein et al. 1992, Yoklavich et al. 2000), which consists of a 2-letter code denoting a primary substratum with >50% coverage of the seafloor and a secondary substratum with 20–49% coverage of the seafloor. Nine identified substratum types were identified using the Wentworth Scale (Wentworth 1922): mud, sand, gravel, pebble (diameter ≤ 6.5 cm), mixed coarse material, cobble (6.5 cm < diameter < 25.5 cm), boulder (diameter > 25.5 cm), exposed low-relief bedrock, and exposed high-relief bedrock. By this classification, a section of seafloor covered primarily in cobble but with boulders over more than 20% of the surface would receive the substratum code cobble–boulder. The substratum code was changed only if a substratum encompassed more than 10 sequential images. The substrate category for each image then was grouped into one of 2 major categories: unconsolidated (mud, sand, pebble, gravel, or mixed coarse substrates) or rock and cobble (cobble, boulder, high and low-relief bedrock) classifications. The proportion of rock and cobble for a transect was computed from the number of images classified as rock and cobble (primary or secondary classification) for the transect divided by the total number of images for the transect. This proportion then was used as an environmental variable in the analysis (proportion of rock and cobble). Unfortunately, no Alaska-wide spatial prediction (raster layer) is available for the proportion of rock and cobble, so while we used this variable to identify the environmental variables structuring assemblages (our second objective), we excluded it from predicting spatial distributions of these assemblages and their indicator taxa (our third objective).

The remaining environmental variables were derived from spatial predictions (raster layers) developed for Alaska and used in previous deep-sea coral and sponge modeling studies (Rooper et al. 2014, 2017, Sigler et al. 2015). For each environmental variable, the raster-layer value at the midpoint of each camera deployment was used in the analysis. A 100 × 100 m bathymetry raster was used (see Zimmermann et al. 2013, Zimmermann & Benson 2013, Zimmermann & Prescott 2015 for details of the bathymetry layers used). This raster was used for prediction (since it had complete coverage of the study area) but not for parameterizing the models. Two environmental variables were derived from the bathymetry raster. Slope for each raster grid cell was computed as the maximum difference in angle (range: 0–90°) between the depth at a cell and its surrounding cells. TPI was calculated from the bathymetry layer as the difference between the depth of a cell and the depth of its surrounding neighbors. This variable was meant to represent the degree to which cells were on peaks or valleys compared to surrounding depths. Slope and TPI were computed using the 'raster' package in R software (Hijmans et al. 2019).

Water movement is important to deep-sea corals and sponges for nutrient delivery, reproduction, and other processes. Water movement in Alaska can be dominated by more dynamic tidal currents as in the Aleutian Islands (Ladd et al. 2005) or underlying and persistent larger scale oceanographic currents as on the Bering Sea slope (Stabeno et al. 1999). Three measures of water movement and their potential interaction with the seafloor were used as environmental variables. The first variable was maximum tidal speed (cm s^{-1}). Tidal speeds were estimated for 368 consecutive days (1 January 2009 to 3 January 2010) using a tidal inversion program parameterized for Alaska on a 1 × 1 km grid (Egbert & Erofeeva 2002). This tidal prediction model was used to produce a time series of one lunar year of tidal currents for spring and neap cycles on a regular grid for each region; the maximum of each time series was computed and the values interpolated to a 100 × 100 m grid using ordinary kriging (Laman et al. 2018).

The second water movement variable was the predicted bottom water layer current speed (m s^{-1}) from Regional Ocean Modeling System (ROMS) model runs from 1970–2004 (Danielson et al. 2011, Her-

mann et al. 2013), with 10 × 10 km grid cells. This 3-dimensional model has 60 depth tiers for each grid cell. A point at 60 m water depth would have 60 depth bins at 1 m intervals, while a point at 120 m depth would have 60 depth bins at 2 m depth intervals, etc. The current speed for the deepest depth bin at each point (closest to the seafloor) was used in this analysis. These regularly spaced data were interpolated to a 100 × 100 m cell size raster using inverse distance weighting. Two different methods (inverse distance weighting and ordinary kriging) were used to interpolate the environmental data because the data were originally derived from different sources with either regular or irregular grid sizes.

The third water movement variable was aspect, computed from the angle of the seafloor relative to the mean current direction. The angle the seafloor faces was computed from the bathymetry layer, in degrees relative to north (0°), using the 'raster' package in R software (Hijmans et al. 2019). The current direction used was output from the ROMS model described above. Aspect is the absolute value of the difference between the current direction and the angle the seafloor faces at each 100 × 100 m grid cell. This value ranged from 0° (where the current was flowing in the same direction the seafloor was facing) to 180° (where the mean current was flowing opposite the direction the seafloor was facing).

The average summer temperature (°C) at each site was estimated from data collected during Alaska bottom trawl surveys from 1991–2018 in the eastern Bering Sea, Aleutian Islands region, and Gulf of Alaska. Bottom temperatures are collected during each bottom trawl tow using the SBE-39 attached to the headrope of the net. Mean bottom temperatures for each haul were interpolated to the 100 × 100 m grid for the regions. These data were interpolated using ordinary kriging (Venables & Ripley 2002). This resulted in a raster layer of average summer bottom temperature from 1991–2018.

A measure of ocean primary productivity (mg C m^{-2} d^{-1}) was computed based on moderate resolution imaging spectroradiometer (MODIS) ocean color data for 5 spring–summer months (May–September) that encompass the spring and summer phytoplankton blooms over 10 yr (2002–2011) for Alaska (Behrenfeld & Falkowski 1997). Surface primary productivity was included in the analyses to reflect the spatial differences in ocean productivity throughout Alaska. We assumed that the productivity available to the benthos would be related to the productivity in the overlying water column. These data were downloaded from Oregon State University's Ocean Productivity website (http://sites.science.oregonstate.edu/ocean.productivity/index.php). The native resolution was 1/6° latitude and longitude. These data were averaged by cell and by month and then averaged again by cell and by year (to account for differences in the number of samples within each cell). The averages were then interpolated to a 100 × 100 m raster grid using inverse distance weighting.

2.4. Analytical methods

2.4.1. Identify deep-sea coral and sponge assemblages

Cluster analysis was used to partition the deep-sea coral and sponge data and identify the major deep-sea coral and sponge assemblages in Alaska (Borcard et al. 2018). The cluster analysis was conducted using the 'stats' package in R. We grouped sites based on similarity of taxa. We considered excluding scarce taxa from the cluster analysis but did not because only one of the 12 taxa analyzed had an FO < 0.01 (i.e. only one group was scarce: Antipatharia, FO = 0.004) (see Table 2). The data were chord transformed (site sum of squares equals 1), which expresses the data as relative abundances per site and removes total abundance per site (the response of the taxon to the total productivity of the sites) (Borcard et al. 2018). Euclidean distances were computed between sites using the relative abundance data.

We applied 2 clustering methods: hierarchical cluster analysis with Ward's minimum variance method and a non-hierarchical method, *k*-means, to optimize Ward's classification (Borcard et al. 2018) (Table 1). In the *k*-means optimization of Ward's classification, the mean taxa values for each of the clusters from Ward's classification were used as a starting point for the *k*-means optimization, and the sum of the squared Euclidean distances within the groups was minimized. Following completion of the cluster analysis, relative abundances for the 12 taxa were plotted by cluster to depict taxa associations and identify indicator taxa for each cluster.

In the hierarchical cluster analysis, we determined the number of clusters based on silhouette width (a measure of how well a site is clustered) and species fidelity analysis (a measure of how well a cluster is characterized by a set of indicator species) (Borcard et al. 2018). The silhouette width is based on the average dissimilarity between a site and all sites of the cluster to which it belongs, compared to the same measure computed for the next closest cluster; sil-

Table 1. Purpose and method as well as the form of the environmental and species data used in each analysis

Purpose	Method	Environmental data	Species data
Identify assemblages	Hierarchical cluster analysis (Borcard et al. 2018)	None	Relative abundance of all (12) taxa
	k-means optimization of cluster analysis (Borcard et al. 2018)	None	Relative abundance of all (12) taxa
Identify environmental variables structuring assemblages	Canonical correspondence analysis (ter Braak 1986)	Values (untransformed)	Abundance (untransformed) of all (12) taxa
Predict spatial distributions of assemblages	Random forest modeling (Cutler et al. 2007)	Values (untransformed)	Presence–absence of clusters
	Generalized additive modeling (Hastie & Tibshirani 1990)	Values (untransformed)	Presence–absence of indicator taxa

houette widths range from −1 to 1 (Borcard et al. 2018). The optimal number of clusters is the number that maximizes the average silhouette width. Species fidelity analysis is based on the concepts of specificity (highest when the species is present in the target group but not elsewhere) and fidelity (highest when the species is present in all sites of the target group). We applied the Dufrêne & Legendre (1997) IndVal index available in the R package 'labdsv', which is a function of specificity and fidelity. The optimal number of clusters is the number that maximizes the IndVal index.

2.4.2. Identify the environmental variables structuring these assemblages

We used canonical correspondence analysis (CCA) (ter Braak 1986) to identify the primary environmental variables structuring deep-sea coral and sponge assemblages in Alaska (Table 1). Our CCA compared the deep-sea coral and sponge data (12 taxa; see Table 2) to the 9 environmental variables. In this sense, the deep-sea coral and sponge data set is the response matrix and the environmental data set is the explanatory matrix. The CCA was conducted using the 'vegan' package in R. The use of CCA should be limited to situations where rare species are well sampled and are seen as potential indicators of particular characteristics of an ecosystem (Borcard et al. 2018). In our data set, only one taxon was rare (FO < 0.01; see Table 2) and taxa were well sampled with the data set consisting of over 850 transect locations. The taxa data are the raw, untransformed abundances in CCA. CCA results were tested by permutation, which, combined with a variable selection process (the 'ordistep' function in the 'vegan' package), was used to find the most parsimonious relationships between the environmental and deep-sea coral and sponge data sets. We displayed the relationships in a biplot. In the biplot, arrows for related environmental variables point in the same general direction, representing a gradient from low values (arrow base) to high values (arrow point). Taxa are located in the biplot along the environmental gradient at their mean position weighted by abundance, so taxa occurring near the point of a variable arrow are positively influenced (more abundant) by that environmental variable.

2.4.3. Predict the spatial distributions of these assemblages

We predicted the spatial distributions of the assemblages (either the identified clusters or the indicator taxon that represents each identified cluster) using 2 methods: random forest models and generalized additive models (GAMs). The random forest model is a multivariate method and was used to predict the presence–absence of each assemblage simultaneously (i.e. one prediction map for all identified clusters, with each grid location assigned to one and only one of the identified clusters). GAMs are a univariate method and were used to predict the presence probability of the indicator taxa for each assemblage individually (i.e. 6 prediction maps with one map for each indicator taxa).

A random forest model is a classification tree-based method (Breiman 2001, Cutler et al. 2007). Random forest models bootstrap the data and fit many individual trees to the bootstrapped data. A random selection of explanatory variables to consider at each split (branch) of the tree is chosen and then the predictions of the multiple resulting trees are combined into a single prediction by ensembling.

Our random forest model was a single multinomial random forest model that related the presence–absence values for the identified clusters to the environmental variables. The analysis included the identified clusters (e.g. Demospongiae) plus a category for sites with no deep-sea coral or sponge present. We created a single multi-class confusion matrix for the clusters. The random forest modeling was conducted using the 'randomForest' package in R. Default values for the number of variables randomly sampled as candidates at each split (n = 3) were used, and the number of trees computed was 5000. In random forest analysis of presence–absence data, the default probability threshold for presence in a group is $1/k$, where k is the number of groups (clusters) (James et al. 2013).

A GAM (Hastie & Tibshirani 1990) is a multiple regression method in which part of the linear predictor is specified in terms of smooth functions of predictor variables (Wood 2006), which allows complex and non-linear relationships to be estimated. Our GAM compared the presence–absence of the indicator taxa identified in the cluster analysis (6 taxa; see Table 2) to the 9 environmental variables. The 'mgcv' package in R (Wood 2006) was used to predict the dependent variables with the suite of untransformed environmental variables included so that the full model was as follows:

$$y = \text{s(depth)} + \text{s(temperature)} + \text{s(slope)} + \text{s(TPI)} + \text{s(maximum tidal current)} + \text{s(mean current speed)} + \text{s(aspect)} + \text{s(ocean color)} + \text{s(proportion of rock and cobble)} + \text{offset[log(area)]} + \varepsilon$$

where y is the dependent variable presence or absence for each indicator taxa and s indicates a thin plate regression spline smoothing function (Wood 2006). In each case, the basis degrees of freedom used in the smoothing function was limited to ≤4. The seafloor area observed at a transect location was treated as a model 'offset'; that is, as a column of the model matrix with the associated parameter fixed at 1 to account for differences in area among transect locations (Wood 2006). A binomial distribution was used for the fitting of these presence–absence models.

Automatic term selection using 'shrinkage' (Marra & Wood 2011) was used to reduce the number of variables in each model, implemented as the 'select' option of the 'mgcv' function 'gam' (Wood 2022). If 'select' is TRUE, then an extra penalty is added to each term so that it can be penalized to zero. This means that the smoothing parameter estimation that is part of fitting can completely remove terms from the model. If the corresponding smoothing parameter is estimated as zero, then the extra penalty has no effect. The outcome of automatic term selection was checked by specifying the reduced model in R and then fitting the reduced model to the data to verify that the results were similar for automatic term selection and the reduced models and that the unbiased risk estimator (UBRE) value was minimized. We also tested backward selection by sequentially removing the variable with the highest p-value in each step but found that this method did not reliably reach the same reduced set of variables as found for the shrinkage method or the lowest UBRE score. For each data set, the model with the lowest UBRE score was deemed the best-fitting model and was used for spatial prediction.

For both random forest models and GAMs, spatial predictions of clusters (random forest) and indicator taxa (GAMs) were made. The raster layers of each of the environmental variables were used in the spatial predictions, except for the proportion of rock and cobble, which has no raster layer for Alaska. For spatial predictions, we used raster layers at a coarser 1 × 1 km grid to speed prediction computation and plotting.

2.4.4. Evaluate predictive models

Model validation and testing was performed by 5-fold cross-validation with spatial partitioning (Valavi et al. 2019) for both random forest models and GAMs. The data were partitioned into $k = 5$ parts (folds), using one part for testing and the remaining ($k - 1$ folds) for model fitting. In 5-fold cross-validation, the process is iterated until all 5 folds have been used for testing. The spatial partitions separate units of geographical area (Valavi et al. 2019). In each iteration, model parameters were estimated with the training data (4 folds), and the model was tested against the held-back data (1 fold). A misclassification table ('confusion matrix') was produced, displaying the number of predictions that matched the corresponding observations as well as those that did not (i.e. how many observations of presence were correctly predicted as presence and how many were incorrectly predicted as absence). Two misclassification tables were produced; one using the test data set and the other using the training data set (both use the best-fitting model based on the training data set).

For random forest modeling, the misclassification table is a measure of the ability of the random forest model to correctly predict the observed classification.

The classification error rate is the proportion that are incorrectly classified. Another evaluation measure can be obtained from the bootstrapped subsets of the observations and the out-of-bag (OOB) subset; one can predict the response for the i^{th} observation using each of the trees in which that observation was OOB, from which the overall OOB classification error can be computed (James et al. 2013). We report the average value of the 5 iterations for each test statistic (e.g. average OOB classification error).

For GAMs, the predictions were compared to the observations by 3 diagnostic methods. The first diagnostic method, the area under the receiver operating characteristic curve (AUC), calculates the probability that a randomly chosen presence observation would have a higher probability of presence than a randomly chosen absence observation, using rank data. AUC > 0.5 is estimated to be better than chance, AUC > 0.7 is estimated to be acceptable, and values >0.8 and 0.9 are excellent and outstanding, respectively (Hosmer & Lemeshow 2005). The threshold probability that balanced the rate of false positive and false negative predictions was used to produce a matrix of presence or absence predictions. From this matrix, we calculated the second diagnostic method, the true skill statistic (TSS; Allouche et al. 2006). Sensitivity is the probability that the model will correctly classify a presence. Specificity is the probability that the model will correctly classify an absence. TSS is calculated from sensitivity and specificity and ranges from −1 to +1, where +1 indicates perfect agreement and values of zero or less indicate a performance no better than random (Allouche et al. 2006). The third diagnostic method, Tjur's coefficient of discrimination (D), is interpreted as the difference between the averages of fitted values for presence and absence and has been recommended for use as a standard measure of explanatory power for presence–absence models (Tjur 2009). A value of D = 0.2 would mean that presences were predicted to have on average a 0.2 higher probability than absences. D is not a true R^2 but is a pseudo-R^2 that is related to the R^2 (Tjur 2009). We report the average value of the 5 iterations for each test statistic (e.g. average AUC for the test data set for Demospongiae).

3. RESULTS

A total of 853 sites were sampled with stereo drop-cameras in the eastern Bering Sea, Aleutian Islands region, and Gulf of Alaska (Fig. 1). Demospongiae was the most common taxa (FO = 0.54, i.e. observed at 54% of the sites) and where observed, the most abundant (average density = 1615 ind. ha^{-1}) (Table 2). Other common taxa (FO > 0.1) were Hexactinellida, *Balticina* sp., Primnoidae, Plexauridae, and Stylasteridae.

Table 2. Observations of corals, sponges, and sea whips and sea pens in underwater camera surveys of the eastern Bering Sea, Aleutian Islands region, and Gulf of Alaska. Taxa were classified into 12 mutually exclusive groups (the finest consistently identified taxa). Proportion non-zero is the proportion of observations (n = 853) with the taxa present (i.e. density greater than zero). The number of observations with at least 1 taxon present was 616. Average density was computed from these observations and is expressed as number per hectare (i.e. a 100 × 100 m square). The constituents of the finest consistently identified taxa are shown; these constituents are the taxa identifications from the post-cruise image analysis. Percentages are based on density

Finest consistently identified taxa	Proportion non-zero	Average density for non-zero observations	Constituent taxa and their percentages
Demospongiae[a]	0.540	1614.6	Demospongiae 100%
Hexactinellida[a]	0.279	72.4	Hexactinellida 100%
Balticina sp.[a]	0.271	384.2	*Balticina* sp. 100%
Primnoidae[a]	0.250	982.8	Primnoidae 64%
			Arthrogorgia sp. 3%
			Fanellia sp. 5%
			Plumarella aleutiana 0.1%
			Plumarella sp. 27%
			Primnoa pacifica 0.01%
			Thouarella sp. 1%
Plexauridae	0.184	163.9	Plexauridae 67%
			Alaskagorgia aleutiana 7%
			Muriceides sp. 22%
			Swiftia sp. 4%
Stylasteridae[a]	0.184	787.3	Stylasteridae 100%
Ptilosarcus gurneyi[a]	0.098	235.8	*Ptilosarcus gurneyi* 100%
Acanthogorgiidae	0.082	63.4	Acanthogorgiidae 81%
			Acanthogorgia sp. 0.04%
			Calcigorgia sp. 19%
Paragorgiidae	0.047	7.4	*Paragorgia* sp. 100%
Isididae	0.023	8.6	Isididae 100%
Calcarea	0.019	0.7	Calcarea 100%
Antipatharia	0.004	0.1	Antipatharia 100%

[a]Indicator taxa from the cluster analysis

3.1. Assemblages

We identified 6 clusters in the deep-sea coral and sponge data. Average silhouette width, a measure of how well a site is clustered, was 0.69 (range: 0.47–0.73) in the final model (*k*-means optimization of Ward's clustering) and was maximized for 6 clusters. The indicator value index, a measure of how well a cluster is characterized by a set of indicator taxa, was maximized for 2 clusters. We chose 6 rather than 2 clusters because for 6 clusters, each cluster had an obvious indicator taxon: *Balticina* sp., Demospongiae, Hexactinellida, Primnoidae, *Ptilosarcus gurneyi*, or Stylasteridae, and we used these taxa names to label the clusters (Fig. 2). These taxa were good indicators because their relative abundance was con-

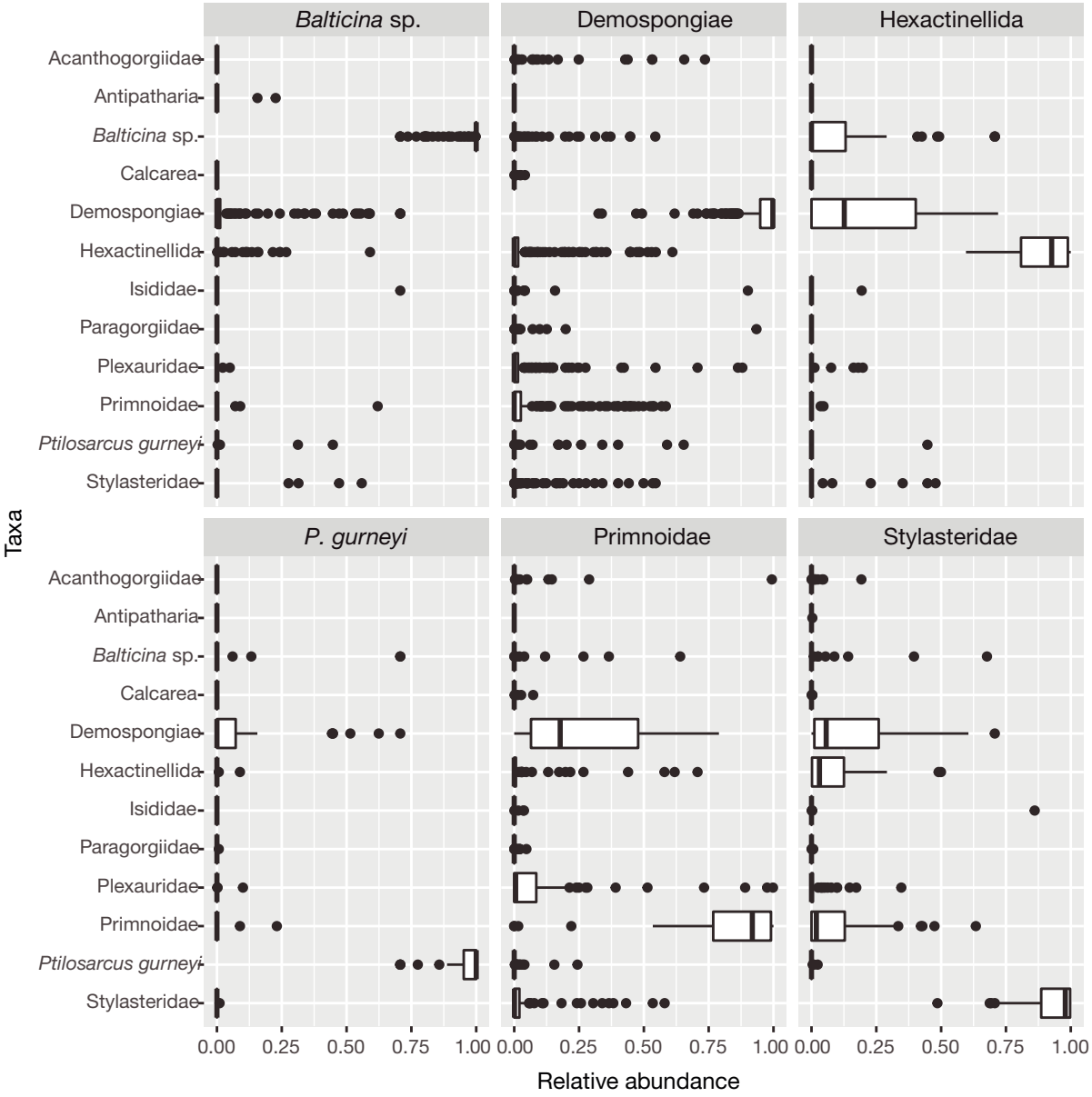

Fig. 2. Relative abundance of the 12 taxa by cluster membership. Each plot shows a cluster with the horizontal axis representing relative abundance (0–1) and the vertical axis representing taxa. Each of the 6 clusters had an obvious indicator species: *Balticina* sp., Demospongiae, Hexactinellida, *Ptilosarcus gurneyi*, Primnoidae, and Stylasteridae, and we used these taxa names to label the clusters. Boxplots extend from 1st to 3rd quartile; median is the heavy line dividing the box; upper whiskers extend from 3rd quartile to largest value no further than 1.5 × IQR from the 3rd quartile (where IQR is the inter-quartile range, or distance between 1st and 3rd quartiles). Lower whiskers extend from 1st quartile to smallest value at most 1.5 × IQR from the 1st quartile. Dots show outliers and are plotted individually

sistently high within their respective cluster (i.e. the median value was at or near 1.0 on a scale of 0–1 for all clusters). These 6 indicator taxa also were among the top 7 most frequently occurring taxa (Table 2). Although clusters were well defined by their respective indicator taxa, other taxa co-occurred within an identified cluster. For example, within the Primnoidae cluster, 2 other taxa were common: Demospongiae and Plexauridae (Fig. 2). However, the median relative abundance of the co-occurring taxa never exceeded 0.2, much lower than the median relative abundance of the indicator taxa of about 1.0.

3.2. Environmental relationships structuring assemblages

The most parsimonious relationship between the environmental and deep-sea coral and sponge (12 taxa; Table 2) data sets included all 9 environmental variables ($p < 0.05$), based on CCA (Fig. 3). The included environmental variables accounted for 31.0% of the variability in the deep-sea coral and sponge data (adjusted R^2). The 6 indicator taxa identified in the cluster analysis (Demospongiae, Primnoidae, etc.) also were distinguished in the CCA (i.e. were spatially separated in the biplot; Fig. 3). The 2 closest taxa spatially were Demospongiae and Primnoidae, which aligned along greater maximum tidal current, bottom current, proportion of rock and cobble, and bottom temperature. *Balticina* sp. was positively influenced in the opposite direction and was aligned along lower maximum tidal current, bottom current, proportion of rock and cobble, and bottom temperature as well as greater depth. Hexactinellida and Stylasteridae aligned differently, toward greater aspect and ocean color. The farthest taxon spatially was *Ptilosarcus gurneyi*, which aligned along greater TPI and lower aspect.

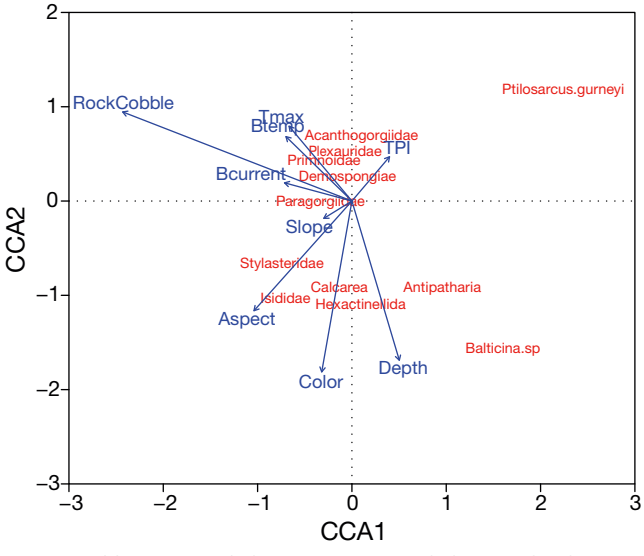

Fig. 3. Alignment of the environmental data and relationships with the taxa (12 taxa; Table 2) data, based on canonical correspondence analysis (CCA). The major CCA axes in the biplot are the first principal component (CCA1) and the second principal component (CCA2). In the biplot, arrows for related environmental variables point in the same general direction and a taxon found along an environmental variable arrow is positively influenced (more abundant) by that environmental variable. The environmental variables are aspect (angle), depth (m), bottom current (Bcurrent, m s^{-1}), average summer bottom temperature (Btemp, °C), average spring–summer ocean color (Color, mg C m^{-2} d^{-1}), slope (angle), maximum tidal current (Tmax, cm s^{-1}), proportion of rock and cobble (RockCobble), and topographic position index (TPI, m)

The proportion of rock and cobble was an important environmental variable for differentiating clusters (Fig. 4) and related taxa had similar preferences. The coral (Primnoidae and Stylasteridae) clusters typically occurred in the areas with the highest proportion of rock and cobble, the sea whip *P. gurneyi* and the sea pen *Balticina* sp. clusters occurred in areas of unconsolidated sediments (proportion of rock and cobble = 0), and the sponge (Hexactinellida and Demospongiae) clusters occurred in low to intermediate proportions of rock and cobble. For these related taxa, pairwise taxa comparisons of the proportion of rock and cobble were not significantly different (ANOVA: Stylasteridae and Primnoidae, $p > 0.99$; *P. gurneyi* and *Balticina* sp., $p = 0.62$; Demospongiae and Hexactinellida, $p = 0.06$). For less related taxa (e.g. Primnoidae and Demospongiae), all pairwise comparisons were significantly different (ANOVA, $p < 0.001$) except for one pair (*P. gurneyi* and Hexactinellida, $p = 0.86$), indicating that Hexactinellida frequently occur at sites with a low proportion of rock and cobble (Fig. 4).

The Primnoidae and *P. gurneyi* clusters were typically found within a narrow shallow depth range (ANOVA, $p = 0.97$). Stylasteridae, likewise, were found at a shallow but wider depth range, similar to Primnoidae ($p = 0.77$) and *P. gurneyi* ($p = 0.49$). The remaining pairwise taxa comparisons were statistically significant ($p < 0.05$) except for Hexactinellida and *Balticina* sp., both found over a deep and wide depth range ($p = 0.97$), and Stylasteridae and Demospongiae, both found at intermediate depths ($p = 0.61$). Primnoidae were found at the highest tidal currents, followed by *P. gurneyi* (ANOVA, $p = 0.10$); Primnoidae was significantly different from all other pairwise comparisons ($p < 0.05$) but *P. gurneyi* was not ($p > 0.16$).

3.3. Predict the spatial distributions of these assemblages

In random forest analysis of presence–absence data, we found that the default threshold of $1/k$, where k is the number of groups (clusters), disproportionately misidentified the Primnoidae cluster as the Demospongiae cluster, so we halved the threshold for the Primnoidae cluster to balance the misidentification rate for the Primnoidae cluster as the Demospongiae cluster and vice versa at about 25%. Class error rates for the training sets averaged about

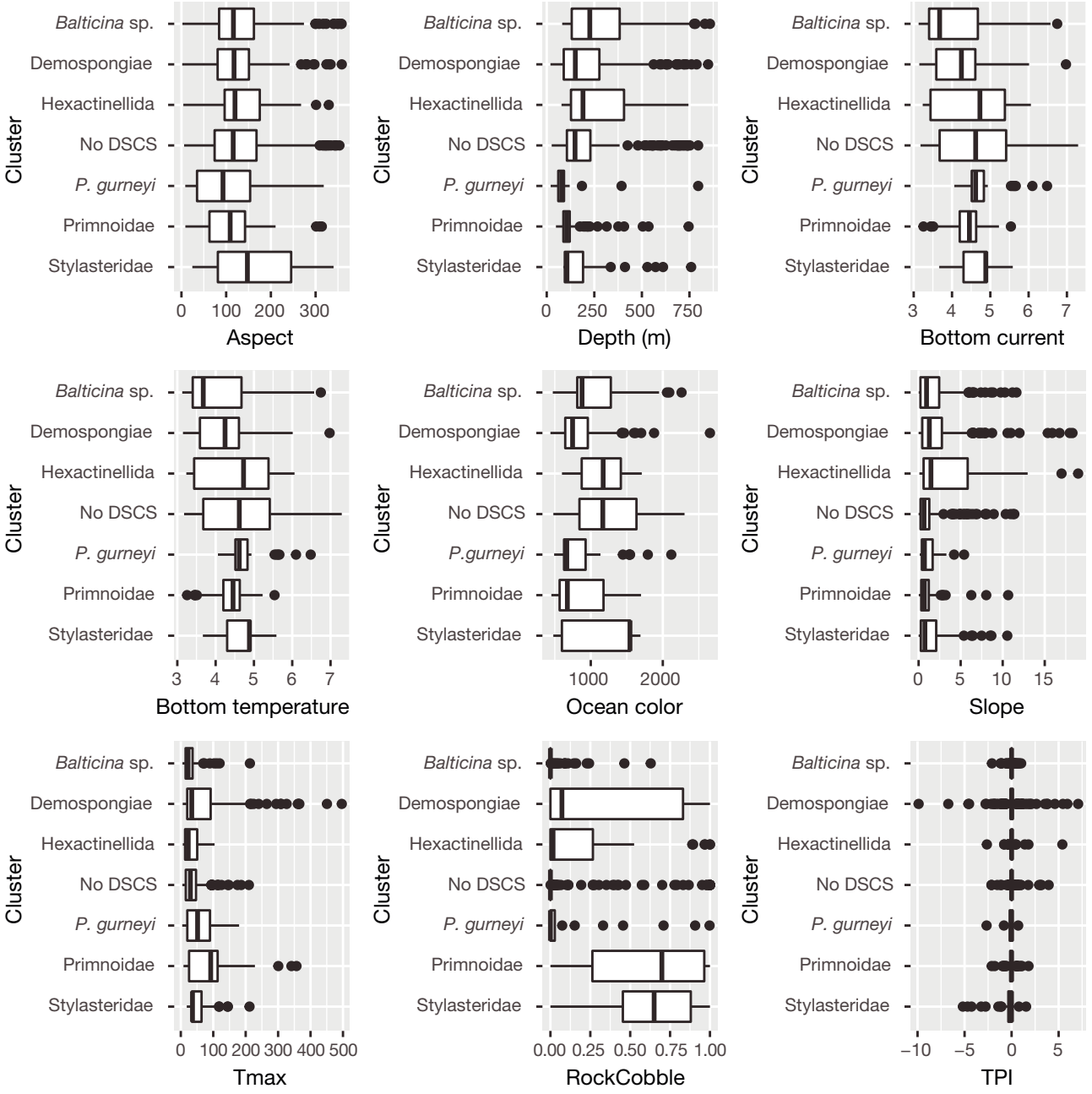

Fig. 4. Values of the environmental variables by cluster. Each plot shows an environmental variable, with the horizontal axis representing values of the environmental variable and the vertical axis representing cluster: aspect (angle), depth (m), bottom current (m s^{-1}), average summer bottom temperature (°C), average spring–summer ocean color (mg C m^{-2} d^{-1}), slope (angle), maximum tidal current (T_{max}, cm s^{-1}), proportion of rock and cobble (RockCobble), and topographic position index (TPI, m). Each of the 6 clusters had an obvious indicator species: *Balticina* sp., Demospongiae, Hexactinellida, no deep-sea coral or sponge (No DSCS), *Ptilosarcus gurneyi*, Primnoidae, and Stylasteridae, and we used these taxa names to label the clusters. See Fig. 2 for explanation of boxplot parameters

30–50% for all clusters except for the Hexactinellida cluster and the *P. gurneyi* cluster, which were 86 and 68%, respectively (Table 3). For the testing sets, average class error rates increased compared to the average values for the training sets, implying some model overfitting. Whether or not the proportion of rock and cobble was included in the analysis had little effect on model performance; the OOB classification error was 45% for the full model and 46% for the reduced model excluding the proportion of rock and cobble. This detail on model performance matters for predicting cluster locations (see next paragraph) because raster layers exist for all of the environmental variables except the proportion of rock and cobble.

In the random forest model, commonly predicted clusters were Demospongiae, the coral taxa Primnoidae, and the sea whip taxa *Balticina* sp. (Fig. 5). Primnoidae, which prefer rock and cobble, primarily occurred in the Aleutian Islands region and the western Gulf of Alaska shelf. Demospongiae were more widespread and mostly concentrated in the Aleutian Islands region and the northwest shelf of the eastern Bering Sea and also scattered along the shelf break of the Gulf of Alaska. *Balticina* sp., which prefers unconsolidated sediment, were widely scattered and mainly concentrated on the outer shelf of the eastern Bering Sea as well as along the shelf break of the Gulf of Alaska.

In the GAMs, the measures of model predictive performance imply that 5 of the 6 estimated relationships are well supported, with *Balticina* sp. being the only exception. The values for the training AUC (average of the 5-fold cross-validation) imply that 5 of the 6 estimated relationships are excellent (>0.8) and even the poorest estimated relationship is acceptable (>0.7, *Balticina* sp.) (Table 3). Likewise, the test AUC values imply that 4 of the 6 estimated relationships are excellent, one is acceptable (Hexactinellida) and even the poorest estimated relationship is better than average (>0.5, *Balticina* sp.) (Table 3). The 2 other measures of model performance (TSS and *D*) imply well-estimated relationships for 5 of 6 indicator taxa, with the exception again being *Balticina* sp. The training TSS values ranged from about 0.5–0.8 except for *Balticina* sp. (~0.3) and the test TSS values ranged from about 0.3–0.6, again except for *Balticina* sp. (0.06). The training *D* values ranged from about 0.3–0.6 except for *Balticina* sp. (0.11) and the test *D* values ranged from about 0.2–0.4 except for *Balticina* sp. (0.05).

In the GAMs, the most parsimonious relationships between the environmental and indicator taxa data sets included 5 or more of the 9 environmental

Table 3. Random forest modeling and generalized additive modeling (GAM); summary of diagnostics. For random forest modeling, the classification error rate is the proportion of a taxon that is incorrectly classified from the confusion matrix. For the GAMs, the Akaike information criterion (AIC) is an estimator of prediction error and thereby relative quality of statistical models for a given set of data (Wood 2006); an area under the receiver operating characteristic curve (AUC) value >0.5 is estimated to be better than chance, AUC > 0.7 is estimated to be acceptable, and AUC > 0.8 and 0.9 are excellent and outstanding, respectively (Hosmer & Lemeshow 2005). True skill statistic (TSS) ranges from −1 to +1, where +1 indicates perfect agreement and values of zero or less indicate a performance no better than random (Allouche et al. 2006). A value Tjur's coefficient of discrimination (*D*) of 0.2 would mean that presences were predicted to have on average a 0.2 higher probability than absences (Tjur 2009). All rows except the last 2 show diagnostics for models fit with 9 environmental variables; the last 2 rows show diagnostics fit excluding one environmental variable, the proportion of rock and cobble

Diagnostic	*Balticina* sp.	Demospongiae	Hexactinellida	Primnoidae	*Ptilosarcus gurneyi*	Stylasteridae
Random forest						
Classification error train	0.52	0.46	0.86	0.32	0.68	0.52
Classification error test	0.72	0.50	0.95	0.81	0.80	0.79
GAM with RockCobble						
AIC	766.1	672.4	632.0	443.9	294.5	308.5
Train threshold	0.28	0.49	0.28	0.22	0.14	0.23
AUC train	0.69	0.85	0.82	0.91	0.92	0.96
AUC test	0.59	0.82	0.75	0.88	0.82	0.91
TSS train	0.27	0.54	0.48	0.69	0.68	0.78
TSS test	0.06	0.45	0.33	0.60	0.43	0.59
D train	0.11	0.39	0.31	0.49	0.29	0.58
D test	0.05	0.35	0.21	0.43	0.19	0.43
GAM without RockCobble						
AUC train	0.68	0.78	0.75	0.85	0.91	0.92
AUC test	0.54	0.70	0.67	0.72	0.76	0.85

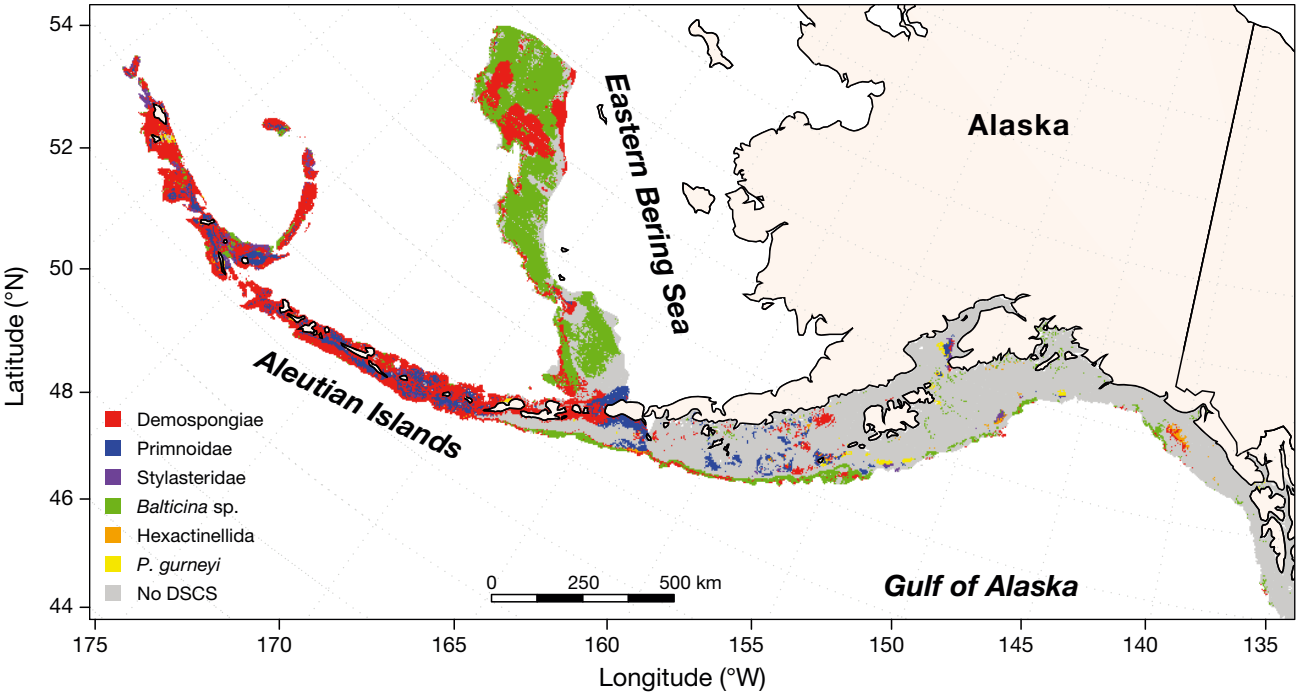

Fig. 5. Random forest model predicting the presence or absence of each cluster for the eastern Bering Sea, Aleutian Islands region, and the Gulf of Alaska. Sponge: Demospongiae, Hexactinellida; coral: Primnoidae; Stylasteridae; sea whip: *Balticina* sp.; Hexactinellida; *Ptilosarcus gurneyi*; no deep-sea corals or sponges present (No DSCS). The random forest model for each dependent variable was applied to the habitat (environmental variable) raster layers to make predictions on a 1 × 1 km grid. Raster layers were available for all environmental variables except proportion of rock and cobble

variables, depending on the indicator taxa (Fig. S1 in the Supplement at www.int-res.com/articles/suppl/m712p067_supp.pdf). *Balticina* sp. were more likely in low current, Demospongiae in intermediate depth, warmer temperature, and higher tidal current, Hexactinellida in greater depth, steeper slope, and an intermediate proportion of rock and cobble, *P. gurneyi* in warmer temperature, Primnoidae in higher tidal current and higher proportion of rock and cobble (>0.5), and Stylasteridae in intermediate ocean color and higher proportion of rock and cobble. Excluding the proportion of rock and cobble from the analysis had little effect on model performance. AUC values for the GAMs were lower, but not by much, for the reduced model (excluding the proportion of rock and cobble) compared to the full model (with all 9 environmental variables) (Table 3).

In the GAMs, *Balticina* sp., which prefers unconsolidated sediment, were widespread and found along the shelf break of the Aleutian Islands region, eastern Bering Sea, and Gulf of Alaska (Fig. S2). *P. gurneyi*, which also prefers unconsolidated sediment, instead were concentrated in the Aleutian Islands region. Demospongiae were concentrated in the Aleutian Islands region, western Gulf of Alaska, and along the shelf break of the Gulf of Alaska. The spatial distribution of Hexactinellida was similar but was found at deeper depths than Demospongiae. Primnoidae, which prefers rock and cobble, primarily occurred in the central and eastern Aleutian Islands region and in the western Gulf of Alaska shelf. Stylasteridae, which also prefers rock and cobble, also was common in the Aleutian Islands region including the western part as well as the shelf break of the central Gulf of Alaska.

4. DISCUSSION

4.1. Ecological interpretation

The assemblages were well defined and influenced by a specific mix of environmental variables. Cluster membership was dominated by a single indicator taxon (Fig. 2), which was true for all 6 clusters. Indicator taxa could spill over into other clusters (e.g. Primnoidae sometimes occurred in the Demospongiae and Stylasteridae clusters), yet their relative abundance usually was low. In the CCA relating taxa to the environmental variables, the 6 indicator taxa were distinct from one another and each aligned along different environmental variables

except for Demospongiae and Primnoidae, which both aligned along the same environmental variables (Fig. 3). In the GAMs used for spatial predictions, most indicator taxa were reliably predicted from the environmental variables. The measures of model predictive performance imply that 5 of the 6 estimated GAM relationships for indicator taxa were well estimated, except *Balticina* sp., which was less defined but still informative (e.g. training AUC, acceptable; test AUC, better than average). The GAMs did a good job of predicting the occurrence of most of the indicator taxa, supporting our conclusion that a specific mix of environmental variables influenced each assemblage.

Deep-sea corals and sponges occupied habitats with a high proportion of rock and cobble, with corals occurring in the rockiest areas and sponges occurring in low to intermediate areas. The exception was sea whips and sea pens, which are known to occupy mostly unconsolidated substrates (Wilborn et al. 2018). Substrate type (especially the presence of hard substrates for attachment of corals and sponges) has been found to be the most important variable determining the presence of these taxa across many ecosystems, including those found in Alaska (Gotelli 1988, Leys & Lauzon 1998, Edinger et al. 2011, Rooper et al. 2016). Depth and current also were important influences in structuring deep-sea coral and sponge assemblages. Primnoidae, Plexauridae, and Acanthogorgiidae co-occurred in shallow, rocky, high-current areas (Fig. 3). Stylasteridae occurred in deeper, rocky areas, and Hexactinellida occurred in deeper, less rocky areas. Both *Ptilosarcus gurneyi* and *Balticina* sp. occurred in soft-bottom areas, with *P. gurneyi* in shallow habitats and *Balticina* sp. in deeper habitats. Demospongiae were common in several clusters and were found in a wide range of habitats, for example with the proportion of rock and cobble ranging from 0–1. The taxonomic resolution of Demospongiae is class, with over 90 identified species and habitat preferences for the Aleutian Islands region (Stone et al. 2011), which likely explains the wide range of habitats occupied.

Clear differences in spatial distributions occurred among the deep-sea corals and sponges. For *Balticina* sp. and *P. gurneyi* (GAM; Fig. S2), which prefer unconsolidated sediment, the former was widespread and occurred in the Aleutian Island region, Bering Sea, and Gulf of Alaska, while the latter was mostly limited to the Aleutian Islands region. Demospongiae and Hexactinellida were concentrated in the Aleutian Islands region, western Gulf of Alaska, and along the shelf break of the Gulf of Alaska, with Hexactinellida found at deeper depths than Demospongiae. Primnoidae and Stylasteridae, which prefer rock and cobble, primarily occurred in the central and eastern Aleutian Islands region, with the latter also common in the western Aleutian Islands region as well as the shelf break of the central Gulf of Alaska. The spatial patterns from the random forest modeling were generally similar to the GAMs but there also were a few differences. In this comparison, we focus on the 3 most common assemblages: *Balticina* sp., Demospongiae, and Primnoidae (Fig. 5). Spatial distributions for both modeling approaches were similar for *Balticina* sp. and Demospongiae, with *Balticina* sp. spread over more of the outer shelf of the Bering Sea for random forest modeling. Both modeling approaches predicted Primnoidae primarily in the Aleutian Islands region, with Primnoidae predicted for the western Gulf of Alaska in random forest modeling but not in GAM.

4.2. Caveats

Most of the environmental variables (slope, bottom temperature, maximum tidal speed, bottom current, ocean color, aspect, TPI) were based on spatial estimates (raster layers) of their average values rather than single measurements coincident with the stereo camera deployments (depth, proportion of rock and cobble). However, deep-sea corals and sponges are long-lived, sessile organisms so average values better represent the environmental conditions they experience rather than one measurement at a single point in time. For example, the bottom temperature variable was based on measurements over 3 decades of summer bottom temperatures from Alaska bottom trawl surveys. In addition, the resolution of the spatial estimates was usually coarser than the scale of the observations (transects averaged a few hundred meters), and the spatial estimates were interpolated to a 100 × 100 m grid. For example, the resolution of the ocean color is 1/24° latitude and longitude (approximately 19 × 9 km) and was interpolated to the 100 × 100 m grid. For ocean surface long-term averages, spatial interpolation of coarse-scale values seems unlikely to add major errors. In contrast, the water movement variables interact with the seafloor and were estimated at coarser resolutions than the 100 × 100 m grid (maximum tidal speed: 1 × 1 km; current speed: 10 × 10 km grid), so fine-scale variation in seafloor topography will introduce some error into values for these 2 water movement variables. For example, the maximum tidal speed at a solitary rock

outcrop will likely be underestimated and, if frequently occurring, make the detection of a statistically significant effect less likely.

The proportion of rock and cobble was an important environmental variable for differentiating clusters, separating sea whips/pens (*Balticina* sp. and *P. gurneyi*) that prefer unconsolidated sediment, coral taxa (Stylasteridae and Primnoidae) that prefer high proportions of rock and cobble, and sponge taxa (Demospongiae and Hexactinellida) that prefer intermediate proportions of rock and cobble. Unfortunately, complete substrate maps do not exist for Alaskan waters, so the proportion of rock and cobble was excluded from predictions of the spatial distributions of deep-sea corals and sponges. However, whether or not the proportion of rock and cobble was included in the analysis had little effect on model performance. For example, a measure of predictive ability for the random forest modeling (the OOB classification error) was similar for the full model (44%) and the reduced model (45%) excluding the proportion of rock and cobble. Likewise, AUC values for the GAMs were lower, but not by much, for the reduced model (excluding the proportion of rock and cobble) compared to the full model (with all 9 environmental variables) (Table 3). At first glance, this is an unexpected result. However, other environmental variables such as maximum tidal current and bottom current are related to the proportion of rock and cobble (Fig. 3). In the reduced model, these other variables were apparently effective proxies for the proportion of rock and cobble and informed predictions of the assemblages and their indicator taxa.

Three coral families in our analysis were compilations of higher resolution taxonomic data. Higher resolution identifications from the post-cruise image analysis (e.g. *Arthrogorgia* sp. from the Primnoidae coral family) sometimes (~⅓ of the time) were available for Primnoidae, Plexauridae, and Acanthogorgiidae, but the grouping usually (~⅔ of the time) matched the highest resolution identification. For example, for the Primnoidae group, the original identifications were Primnoidae 64%, *Arthrogorgia* sp. 3%, *Fanellia* sp. 5%, *Plumarella aleutiana* 0.1%, *Plumarella* sp. 27%, *Primnoa pacifica* 0.01%, and *Thouarella* sp. 1% (Table 2). For the remaining 9 of 12 taxa (e.g. Demospongiae), these were the highest resolution identifications made in the post-cruise image analysis (i.e. Demospongiae was the highest resolution taxonomic data available from the post-cruise image analysis). Overall, most (90%) of the taxonomic groupings in our analysis were the highest resolution taxonomic data available.

One important analysis choice that we made for the deep-sea coral and sponge data was to group (cluster) the data rather than look for gradients. Looking for gradients is done to visualize gradational patterns among species (e.g. Pérez & Ballesteros 2004, Menezes et al. 2006, Tamir et al. 2019) as well as temporal (e.g. Warwick & Clarke 1990) and spatial gradations (e.g. Sigler et al. 2017) and often is combined with cluster analysis (e.g. Pérez & Ballesteros 2004, Menezes et al. 2006, Tamir et al. 2019). Cluster analysis is done to identify groups of stations showing faunal similarities (e.g. Pérez & Ballesteros 2004, Menezes et al. 2006) and to determine the optimal number of communities for subsequent analysis (e.g. Tamir et al. 2019). One reason for choosing cluster rather than gradient analyses was to meet our objective of identifying major Alaskan coral and sponge assemblages. We wondered whether there were distinct communities that could be distinguished from one another, still subject to local environmental characteristics yet distinguishable from one another, similar to the way that elevation and exposure create distinct (terrestrial) mountain plant communities. Another reason for choosing cluster analysis rather than spatial gradient analysis is that a frequent feature of coral and sponge habitat, the proportion of rock and cobble, is often patchy and discontinuous; these spatial discontinuities limit analysis of spatial gradients and thus a clustering approach seems more appropriate.

In the cluster analysis, we employed 2 commonly used measures to determine the number of clusters: silhouette width (e.g. Lechner et al. 2016) and the IndVal index (e.g. Menezes et al. 2006, Tamir et al. 2019). The measures used to determine the number of clusters do not always recommend the same number (Borcard et al. 2018). In our analysis, silhouette width recommended 6 clusters whereas the IndVal index recommended only 2 clusters. We chose 6 rather than 2 clusters because for 6 clusters, each cluster had one obvious indicator taxa, whereas for 2 clusters, multiple indicator taxa were mixed in each cluster.

4.3. Indicator taxa and their use in identifying VMEs

VMEs have been defined as systems that are susceptible to damage by bottom-contacting fishing gear (General Assembly Resolution 64/72; United Nations 2010). Typically, VMEs are identified by the presence of VME indicator species, which are spe-

cies defined as (1) unique or rare, (2) functionally significant as habitat, (3) fragile, (4) long-lived or with episodic or infrequent recruitment, and (5) structurally complex (FAO 2009). This definition is somewhat different from the definition of indicator species typically used in community ecology, where an indicator species is indicative of a certain type of community assemblage (e.g. Dufrêne & Legendre 1997). Here, we utilized the FAO definition of VME indicator species to identify the taxa of concern (deep-sea coral and sponge taxa that are vulnerable to damage by bottom-contact gear) and then used community analyses to identify representative members of VME communities and their spatial distributions for conservation measures. This approach allows identification of VME communities (Watling & Auster 2021) where multiple taxa of VME indicator species are likely to co-occur.

In practice, the VME indicator species approach (FAO 2009) has resulted in broad definitions of indicator taxa for most management bodies (e.g. NPFC 2019, ICES 2020, SPRFMO 2020). For example, in the North Pacific Fisheries Commission, VME indicator taxa are defined as '*Alcyonacea*, *Antipatharia*, *Gorgonacea*, and *Scleractinia*' (NPFC 2019). Within each of these groups, there is large variation in life history traits and subsequent vulnerability to mobile bottom fishing gear. For example, the order *Alcyonacea* contains species such as *Gersemia rubiformis*, which is a low and rapidly growing species and likely less vulnerable than *Primnoa pacifica*, a large and slow-growing species in the same order. In general, similar approaches to managing benthic impacts on corals and sponges based on large taxonomic groupings are the rule within national waters as well (e.g. Wallace et al. 2015, MacLean et al. 2017). Implementing spatial closures based on these larger taxonomic groupings can lead to imprecise management of VMEs. Using community analysis to identify representative members of the VME communities adds management precision and lets managers target protections on communities of vulnerable species indicated by the presence of a single taxonomic group (e.g. Primnoidae).

Several methods have been applied to develop targeted protection of VMEs. Their goal is to simplify taxonomic diversity into VME indicators that identify areas where habitat protections can be most effectively placed. Here, we defined VME indicators based on community analysis and then predicted their spatial distributions using species distribution modeling. In an alternative method with a similar goal, observations of individual taxa themselves or their modeled distributions are assembled into spatial distributions of VMEs by stacking individual species distribution models or observations (Morato et al. 2018, Burgos et al. 2020). This method is especially useful for data from varying sources with uncertainties regarding the sample representativeness or biases in the spatial patterns of observations (Burgos et al. 2020). Species archetype modeling also has been used to generate maps of indicator species where species observations are used to generate clusters of taxa with similar environmental responses and then using mixture models, utilize taxa with stronger data to assist in determining the spatial distribution of taxa with weaker data with the same environmental responses (Murillo et al. 2018).

The approach presented here (community analysis with species distribution modeling of the community indicators) is a data-driven method for identifying both VME indicators and their distributions. This data-driven method is an improvement over approaches that qualitatively define indicators as broad groups of taxa. This method also is less complex and easier to implement than methods that utilize species distribution models across multiple individual taxa with varying levels of data support. These other approaches also often suffer from lumping taxa into groups with a range of life histories and susceptibility to damage by mobile fishing gear. Using quantitative analyses like ours to define VME indicator species allows identification and protection that better targets VME communities.

Our approach led us to identify 6 distinct assemblages, each characterized by a single relatively abundant indicator taxon. These VME indicators can guide the identification of protected areas. Examining the co-occurrence of deep-sea coral and sponge taxa provides a sense of potential effectiveness. For example, protecting the habitat where Primnoidae occur will protect a wide range of taxa (Table 4). Several coral taxa co-occur with Primnoidae at high rates (>75% of each taxon's observations) including Acanthogorgiidae, Isididae, Paragorgiidae, Plexauridae, and Stylasteridae as well as one sponge taxon, Calcarea. Other sponge taxa co-occur at intermediate rates (44 and 53% for Demospongiae and Hexactinellida, respectively). Only the soft-sediment-preferring *Balticina* sp. co-occurs at a low rate (14%). Protecting the habitat where Stylasteridae occur also protects a wide range of taxa, similar to the result for Primnoidae. Protecting the habitat where Demospongiae occur also protects a wide range of taxa, at higher rates than Primnoidae and Stylasteridae. However, Demospongiae were observed twice as

often as Primnoidae (461 vs. 213 of the 853 observations), so reaching this level of protection implies much larger closure areas. In developing ocean management regulations, which is outside the scope of this paper, a cost–benefit analysis would evaluate choices such as these. Such an analysis also would likely examine other metrics besides co-occurrence for evaluating conservation benefits, such as deep-sea coral and sponge density, height, and diversity.

4.4. Conclusions

Deep-sea corals and sponges in Alaska form well-defined assemblages based on their co-occurrence and environmental preferences. We used these characteristics to define indicator taxa for the assemblages and predict their spatial distributions using species distribution models. In combination, these 2 results provide a useful tool for identifying areas of deep-sea coral and sponge habitat in Alaska that would likely benefit from protection from bottom-contacting fishing gear. Monitoring these indicator taxa on a large scale will enable us to track the future health of VMEs in Alaska.

Acknowledgements. We thank all of the vessel companies, ships' crews, and sea-going scientists who collected these data. We thank Al Hermann for providing ROMS model outputs. Data collection was supported by the deep-sea Coral Research and Technology Program at National Oceanic and Atmospheric Administration (NOAA) and the NOAA Alaska Fisheries Science Center–Alaska Regional Office Habitat Research Program. We appreciate the comments of 3 anonymous reviewers, which improved our paper.

LITERATURE CITED

Allouche O, Tsoar A, Kadmon R (2006) Assessing the accuracy of species distribution models: prevalence, kappa and the true skill statistic (TSS). J Appl Ecol 43:1223–1232

Behrenfeld MJ, Falkowski PG (1997) Photosynthetic rates derived from satellite-based chlorophyll concentration. Limnol Oceanogr 42:1–20

Borcard D, Gillet F, Legendre P (2018) Numerical ecology with R, 2nd edn. Springer, New York, NY

Breiman L (2001) Statistical modeling: the two cultures. Stat Sci 16:199–231

Brodeur RD (2001) Habitat-specific distribution of Pacific ocean perch (*Sebastes alutus*) in Pribilof Canyon, Bering Sea. Cont Shelf Res 21:207–224

Buhl-Mortensen L, Vanreusel A, Gooday AJ, Levin LA and others (2010) Biological structures as a source of habitat heterogeneity and biodiversity on the deep ocean margins. Mar Ecol 31:21–50

Burgos JM, Buhl-Mortensen L, Buhl-Mortensen P, Ólafsdóttir SH, Steingrund P, Ragnarsson SÁ, Skagseth Ø (2020) Predicting the distribution of indicator taxa of vulnerable marine ecosystems in the arctic and sub-arctic waters of the Nordic Seas. Front Mar Sci 7:131

Cairns SD (2011) A revision of the Primnoidae (Octocorallia: Alcyonacea) from the Aleutian Islands and Bering Sea. Smithson Contrib Zool 634:1–55

Cimberg RL, Gerrodette T, Muzik K (1981) Habitat requirements and expected distribution of Alaska coral. Final Report No. 54, Research Unit 601, VTN Oregon. Report prepared for the Office of Marine Pollution Assessment, US Dept Commerce, Washington, DC, p 207–308

Clark MR, Rowden AA (2009) Effect of deepwater trawling on the macroinvertebrate assemblages of seamounts on the Chatham Rise, New Zealand. Deep Sea Res I 56: 1540–1554

Cutler DR, Edwards TC Jr, Beard KH, Cutler A, Hess KT, Gibson J, Lawler JJ (2007) Random forests for classification in ecology. Ecology 88:2783–2792

Danielson S, Curchitser E, Hedstrom K, Weingartner T, Stabeno P (2011) On ocean and sea ice modes of variability in the Bering Sea. J Geophys Res 116:C12034

Table 4. Co-occurrence of observations (presence–absence) of corals, sponges, and sea whips in underwater camera surveys of the eastern Bering Sea, Aleutian Islands region, and Gulf of Alaska. For each indicator species, the co-occurrences of the 12 taxa were computed as a percentage. For example, 99% of observed Acanthogorgiidae co-occurred with Demospongiae. Values above 50% are in **bold**. Total number of observations for each taxon is listed in the last row. Total sample size was 853

Indicator species	Acanthogorgiidae	Antipatharia	Calcarea	Demospongiae	*Balticina* sp.	Hexactinellida	Isididae	Paragorgiidae	Plexauridae	Primnoidae	*Ptilosarcus gurneyi*	Stylasteridae
Demospongiae	**99**	**67**	**100**	**100**	49	**90**	**95**	**100**	**100**	**95**	**74**	**94**
Balticina sp.	13	**67**	25	25	**100**	29	25	8	16	15	19	20
Hexactinellida	43	**67**	**81**	46	29	**100**	**80**	43	**53**	**59**	29	**71**
Ptilosarcus gurneyi	31	33	13	13	7	10	10	15	25	19	**100**	17
Primnoidae	**87**	33	**75**	44	14	**53**	**80**	**75**	**79**	**100**	49	**76**
Stylasteridae	**73**	33	**63**	32	14	47	**55**	**80**	**56**	**56**	31	**100**
Number of observations	70	3	16	461	231	238	20	40	157	213	84	157

de la Torriente A, González-Irusta JM, Aguilar R, Fernández-Salas LM, Punzón A, Serrano A (2019) Benthic habitat modelling and mapping as a conservation tool for marine protected areas: a seamount in the western Mediterranean. Aquat Conserv 29:732–750

Dufrêne M, Legendre P (1997) Species assemblages and indicator species: the need for a flexible asymmetrical approach. Ecol Monogr 67:345–366

Edinger EN, Sherwood OA, Piper DJ, Wareham VE, Baker KD, Gilkinson KD, Scott DB (2011) Geological features supporting deep-sea coral habitat in Atlantic Canada. Cont Shelf Res 31:S69–S84

Egbert GD, Erofeeva SY (2002) Efficient inverse modeling of barotropic ocean tides. J Atmos Ocean Technol 19:183–204

FAO (2009) International guidelines for the management of deep-sea fisheries in the High Seas. FAO, Rome

FAO (2016) Vulnerable marine ecosystems: processes and practices in the High Seas. FAO Fisheries and Aquaculture Technical Paper No. 595. FAO, Rome

Ferrier S, Guisan A (2006) Spatial modelling of biodiversity at the community level. J Appl Ecol 43:393–404

Freese JL (2001) Trawl-induced damage to sponges observed from a research submersible. Mar Fish Rev 63: 7–13

Gotelli NJ (1988) Determinants of recruitment, juvenile growth, and spatial distribution of a shallow-water gorgonian. Ecology 69:157–166

Hastie TJ, Tibshirani RJ (1990) Generalized additive models. Chapman & Hall, London

Heifetz J, Stone RP, Shotwell SK (2009) Damage and disturbance to coral and sponge habitat of the Aleutian Archipelago. Mar Ecol Prog Ser 397:295–303

Hermann AJ, Gibson GA, Bond NA, Curchitser EN and others (2013) A multivariate analysis of observed and modeled biophysical variability on the Bering Sea shelf: multidecadal hindcasts (1970–2009) and forecasts (2010–2040). Deep Sea Res II 94:121–139

Hijmans RJ, van Etten J, Sumner M, Cheng J and others (2019) raster: geographic data analysis and modeling. R package version 3.4-13. https://CRAN.R-project.org/package=raster

Hosmer DW, Lemeshow S (2005) Assessing the fit of the model in applied logistic regression, 2nd edn. John Wiley & Sons, Hoboken, NJ

ICES (2020) ICES/NAFO Joint Working Group on Deep-water Ecology (WGDEC). ICES Sci Rep 2:1–188

James G, Witten D, Hastie T, Tibshirani R (2013) An introduction to statistical learning. Springer, New York, NY

Jansen J, Hill NA, Dunstan PK, Eléaume MP, Johnson CR (2018) Taxonomic resolution, functional traits, and the influence of species groupings on mapping Antarctic seafloor biodiversity. Front Ecol Evol 19:6–81

Koslow JA, Gowlett-Holmes K, Lowry JK, O'Hara T, Poore GCB, Williams A (2001) Seamount benthic macrofauna off southern Tasmania: community structure and impacts of trawling. Mar Ecol Prog Ser 213:111–125

Krieger KJ (2001) Coral (*Primnoa*) impacted by fishing gear in the Gulf of Alaska. In: Willison JHM, Hall J, Gass SE, Kenchington ELR, Butler M, Doherty P (eds) Proceedings of the first international symposium on deep-sea corals. Ecology Action Centre, Dalhousie University and Nova Scotia Museum, Halifax, p 106–116

Ladd C, Hunt GL Jr, Mordy CW, Salo SA, Stabeno PJ (2005) Marine environment of the eastern and central Aleutian Islands. Fish Oceanogr 14:22–38

Laman EA, Rooper CN, Turner K, Rooney S, Cooper DW, Zimmermann M (2018) Using species distribution models to describe essential fish habitat in Alaska. Can J Fish Aquat Sci 75:1230–1255

Lechner AM, McCaffrey N, McKenna P, Venables WN, Hunter JT (2016) Ecoregionalization classification of wetlands based on a cluster analysis of environmental data. Appl Veg Sci 19:724–735

Leys SP, Lauzon NRJ (1998) Hexactinellida sponge ecology: growth rates and seasonality in deep water sponges. J Exp Mar Biol Ecol 230:111–129

Linley TD, Lavaleye M, Maiorano P, Bergman M and others (2017) Effects of cold-water corals on fish diversity and density (European Continental Margin: Arctic, NE Atlantic and Mediterranean Sea): data from three baited lander systems. Deep Sea Res II 145:8–21

Love MS, Schroeder DM, Lenarz W, MacCall A, Scarborough Bull A, Thorsteinson L (2006) Potential use of offshore marine structures in rebuilding an overfished rockfish species, bocaccio (*Sebastes paucispinis*). Fish Bull 104:383–390

MacLean SA, Rooper CN, Sigler MF (2017) Corals, canyons, and conservation: science based fisheries management decisions in the eastern Bering Sea. Front Mar Sci 4:112

Marra G, Wood SN (2011) Practical variable selection for generalized additive models. Comput Stat Data Anal 55: 2372–2387

McFadden CS, van Ofwegen LP, Quattrini AM (2022) Revisionary systematics of Octocorallia (Cnidaria: Anthozoa) guided by phylogenomics. Bull Soc System Biol 1:8735

McIntyre FD, Drewery J, Eerkes-Medrano D, Neat FC (2016) Distribution and diversity of deep-sea sponge grounds on the Rosemary Bank Seamount, NE Atlantic. Mar Biol 163:143

Menezes GM, Sigler MF, Silva HM, Pinho MR (2006) Structure and zonation of demersal fish assemblages off the Azores Archipelago (mid-Atlantic). Mar Ecol Prog Ser 324:241–260

Morato T, Pham CK, Pinto C, Golding N and others (2018) A multi criteria assessment method for identifying vulnerable marine ecosystems in the North-East Atlantic. Front Mar Sci 5:460

Moritz C, Lévesque M, Gravel D, Vaz S, Archambault D, Archambault P (2013) Modelling spatial distribution of epibenthic communities in the Gulf of St. Lawrence (Canada). J Sea Res 78:75–84

Murillo FJ, Kenchington E, Tompkins G, Beazley L, Baker E, Knudby A, Walkusz W (2018) Sponge assemblages and predicted archetypes in the eastern Canadian Arctic. Mar Ecol Prog Ser 597:115–135

NPFC (North Pacific Fisheries Commission) (2019) CMM 2019-06 for bottom fisheries and protection of VMEs in the NE Pacific Ocean. https://www.npfc.int/active-conservation-and-management-measures

Pérez RA, Ballesteros LM (2004) Coral community structure and dynamics in the Huatulco area, western Mexico. Bull Mar Sci 75:453–472

Reiswig HM (2020) Report of *Cladorhiza bathycrinoides* Koltun (Demospongiae) from North America and a new species of *Farrea* (Hexactinellidae) among sponges from Cordell Bank, California. Zootaxa 4747:562–574

Rice AL, Thurston MH, New AL (1990) Dense aggregations of the hexactinellida sponge, *Pheronema carpenter*, in the Porcupine Sea bight (northeast Atlantic Ocean), and possible causes. Prog Oceanogr 24:179–196

Rooper CN, Zimmermann M, Prescott MM, Hermann AJ (2014) Predictive models of coral and sponge distribution, abundance and diversity in bottom trawl surveys of the Aleutian Islands, Alaska. Mar Ecol Prog Ser 503: 157–176

Rooper CN, Sigler MF, Goddard P, Malecha P and others (2016) Validation and improvement of species distribution models for structure-forming invertebrates in the eastern Bering Sea with an independent survey. Mar Ecol Prog Ser 551:117–130

Rooper CN, Zimmermann M, Prescott MM (2017) Comparison of modeling methods to predict the spatial distribution of deep-sea coral and sponge in the Gulf of Alaska. Deep Sea Res I 126:148–161

Rooper CN, Wilborn RE, Goddard P, Williams K, Towler R, Hoff GR (2018) Validation of deep-sea coral and sponge distribution models in the Aleutian Islands, Alaska. ICES J Mar Sci 75:199–209

Serrano A, González-Irusta JM, Punzón A, García-Alegre A and others (2017) Deep-sea benthic habitats modeling and mapping in a NE Atlantic seamount (Galicia Bank). Deep Sea Res I 126:115–127

Sigler MF, Rooper CN, Hoff GR, Stone RP, McConnaughey RA, Wilderbuer TK (2015) Faunal features of submarine canyons on the eastern Bering Sea slope. Mar Ecol Prog Ser 526:21–40

Sigler MF, Mueter FJ, Bluhm BA, Busby MS and others (2017) Late summer open water zoogeography of the northern Bering and Chukchi seas. Deep-Sea Res II 135:168–189

SPRFMO (South Pacific Regional Fisheries Management Organization) (2020) CMM 03-2020: conservation and management measure for the management of bottom fishing in the SPRFMO Convention Area. https://www.sprfmo.int/assets/Fisheries/Conservation-and-Management-Measures/2020-CMMs/CMM-03-2020-Bottom-Fishing-31Mar20.pdf (accessed 15 Nov 2022)

Stabeno PJ, Schumacher JD, Ohtani K (1999) The physical oceanography of the Bering Sea. In: Loughlin TR, Ohtani K (eds) Dynamics of the Bering Sea: a summary of physical, chemical, and biological characteristics, and a synopsis of research on the Bering Sea. North Pacific Marine Science Organization (PICES), University of Alaska Sea Grant, AK-SG-99-03, Fairbanks, AK, p 1–59

Stein DL, Tissot BN, Hixon MA, Barss W (1992) Fish-habitat associations on a deep reef at the edge of the Oregon continental shelf. Fish Bull 90:540–551

Stone RP (2014) The ecology of deep-sea coral and sponge habitats of the central Aleutian Islands of Alaska. NOAA Prof Paper NMFS 16. US Department of Commerce, Seattle, WA

Stone RP, Lehnert H, Reiswig H (2011) A guide to the deep-water sponges of the Aleutian Island Archipelago. NOAA Prof Paper NMFS 12. US Department of Commerce, Seattle, WA

Tamir R, Eyal G, Kramer N, Laverick JH, Loya Y (2019) Light environment drives the shallow-to-mesophotic coral community transition. Ecosphere 10:e02839

ter Braak CJF (1986) Canonical correspondence analysis: a new eigenvector technique for multivariate direct gradient analysis. Ecology 67:1167–1179

Tjur T (2009) Coefficients of determination in logistic regression models — a new proposal: the coefficient of discrimination. Am Stat 63:366–372

United Nations (2010) Resolution adopted by the General Assembly on 4 December 2009. A/RES/64/72. https://documents-dds-ny.un.org/doc/UNDOC/GEN/N09/466/15/PDF/N0946615.pdf?OpenElement (accessed 24 November 2022)

Valavi R, Elith J, Lahoz-Monfort JJ, Guillera-Arroita G (2019) BlockCV: an R package for generating spatially or environmentally separated folds for *k*-fold cross-validation of species distribution models. Methods Ecol Evol 10:225–232

Venables WN, Ripley BD (2002) Modern applied statistics with S, 4th edn. Springer Science + Business Media, New York, NY

Vihtakari M (2022) ggOceanMaps: plot data on oceanographic maps using 'ggplot2'. R package version 1.3.7. https://mikkovihtakari.github.io/ggOceanMaps/

Wallace S, Turris B, Driscoll J, Bodtker K, Mose B, Munro G (2015) Canada's Pacific Groundfish Trawl Habitat Agreement: a global first in an ecosystem approach to bottom trawl impacts. Mar Policy 60:240–248

Warwick RM, Clarke KR (1990) A statistical analysis of coral community responses to the 1982–83 El Niño in the Thousand Islands, Indonesia. Coral Reefs 8:171–179

Watling L, Auster PJ (2021) Vulnerable marine ecosystems, communities, and indicator species: confusing concepts for conservation of seamounts. Front Mar Sci 8:622586

Watling L, France SC, Pante E, Simpson A (2011) Biology of deep-water octocorals. Adv Mar Biol 60:41–122

Wentworth CK (1922) A scale of grade and class terms for clastic sediments. J Geol 30:377–392

White M (2003) Comparison of near seabed currents at two locations in the Porcupine Sea Bight — implications for benthic fauna. J Mar Biol Assoc UK 83:683–686

Wilborn R, Rooper CN, Goddard P, Li L, Williams K, Towler R (2018) The potential effects of substrate type, currents, depth and fishing pressure on distribution, abundance, diversity, and height of cold-water corals and sponges in temperate, marine waters. Hydrobiologia 811:251–268

Williams K, Rooper CN, Towler R (2010) Use of stereo camera systems for assessment of rockfish abundance in untrawlable areas and for recording pollock behavior during midwater trawls. Fish Bull 108:352–362

Winship AJ, Thorson JT, Clarke ME, Coleman HM and others (2020) Good practices for species distribution modeling of deep-sea corals and sponges for resource management: data collection, analysis, validation, and communication. Front Mar Sci 7:303

Wood SN (2006) Generalized additive models: an introduction with R. Chapman and Hall/CRC Press, Boca Raton, FL

Wood SN (2022) Mixed GAM computation vehicle with automatic smoothness estimation (Package 'mgcv' version 1.8-39). https://cran.r-project.org/web/packages/mgcv/mgcv.pdf

Yoklavich MM, Greene HG, Cailliet GM, Sullivan DE, Lea RN, Love MS (2000) Habitat associations of deep-water rockfishes in a submarine canyon: an example of a natural refuge. Fish Bull 98:625–641

Zimmermann M, Benson JL (2013) Smooth sheets: how to work with them in a GIS to derive bathymetry, features and substrates. NOAA Tech Memo NMFS-AFSC-249

Zimmermann M, Prescott MM (2015) Smooth sheet bathymetry of the central Gulf of Alaska. NOAA Tech Memo NMFS-AFSC-287

Zimmermann M, Prescott MM, Rooper CN (2013) Smooth sheet bathymetry of the Aleutian Islands. NOAA Tech Memo NMFS-AFSC-250

Editorial responsibility: James McClintock, Birmingham, Alabama, USA
Reviewed by: 3 anonymous referees

Submitted: December 10, 2022
Accepted: April 25, 2023
Proofs received from author(s): May 17, 2023